Surface Science 603 (2009) 641–646

Contents lists available at ScienceDirect

Surface Science

journal homepage: www.elsevier.com/locate/susc

Possible reaction pathway in methanol dehydrogenation on Pt and Ag surfaces/clusters starting from O–H scission: Dipped adcluster model study

Takahiro Watanabe [a], Masahiro Ehara [a,c,*], Kei Kuramoto [a,1], Hiroshi Nakatsuji [a,b,c]

[a] Department of Synthetic Chemistry and Biological Chemistry, Graduate School of Engineering, Kyoto University, Katsura, Nishikyou-ku, Kyoto 615-8510, Japan
[b] Quantum Chemistry Research Institute, Kyodai Katsura Venture Plaza 106, Goryo Oohara 1-36, Nishikyo-ku, Kyoto 615-8245, Japan
[c] JST, CREST, Sanbancho-5, Chiyoda-ku, Tokyo 102-0075, Japan

ARTICLE INFO

Article history:
Received 1 August 2008
Accepted for publication 5 January 2009
Available online 13 January 2009

Keywords:
Ab initio quantum chemical calculations
Dipped adcluster model
Methanol dehydrogenation
Pt surface and cluster

ABSTRACT

The mechanism of the methanol dehydrogenation reaction on a Pt surface has been investigated using the dipped adcluster model (DAM) combined with density-functional theory (DFT) calculations. Starting from O–H bond scission, methanol decomposes to form CO exothermically on the Pt surface, where the Pt-dσ orbital effectively interacts with the O–H antibonding orbital. The donative interaction of the Pt-dσ orbitals was found to be important for catalytic activation on the Pt surface. The reaction pathway starting from C–H bond scission has a larger activation barrier and, therefore, is less kinetically favorable. Electron transfer from the bulk, which is included in the present DAM calculation, plays an important role in the reaction pathway from O–H bond scission, in particular for the dehydrogenation of formaldehyde. On the other hand, the Ag surface has been shown to be effective for formaldehyde synthesis, because formaldehyde desorbs spontaneously from the Ag surface. The present reaction has also been examined and discussed in view of the nanoscale clusters and nanorods.

1. Introduction

The oxidative reaction of methanol on a metal surface is one of the most important catalytic processes in the chemical industry. The production of formaldehyde has been conducted using Ag or Fe/Mo catalysts [1,2]. Recently, the methanol dehydrogenation reaction has received much attention because of its potential application in Direct Methanol Fuel Cells (DMFCs) [3–7]. DMFCs are superior to hydrogen-based fuel cells, because storage and conveyance is much easier for methanol than hydrogen. Taking advantage of these characteristics, DMFCs for mobile electrical products, such as mobile batteries, have been developed.

Many studies have been devoted to the development of DMFCs but commercialization has not been established yet, although prototypes of commercial DMFC units have been publicized. One of the reasons is that a practical catalyst for the oxidative reaction of methanol has not been established. Although it has been recognized that Pt catalysts show high activity for dehydrogenation of methanol to CO [3–5], more efficient decomposition is necessary to generate ample electric power. Poisoning by product CO is also a problem for commercial viability, although alloying with Ru is known to be one of the solutions [3–5]. The present work focuses on the methanol decomposition reaction on the Pt surface of DMFC, but the theoretical model mainly describes the reaction under vacuum condition, a solid/vacuum interface.

For the methanol dehydrogenation reaction, two types of reaction pathways have been proposed experimentally, as shown in Fig. 1. One possibility is a route that starts from scission of the O–H bond, followed stepwise by scission of the C–H bond [8]. The other possible route starts from C–H bond scission [9]. Many experiments, most of which are based on spectroscopic measurements, have been done to elucidate the mechanism of this reaction. However, the reaction mechanism is still unclear in particular for the first dehydrogenation step. This is partly because the high reactivity of the Pt catalyst prevents us from directly observing the intermediates and other related compounds. It has been reported that detection of the metastable intermediate species is difficult, except for methanol, CO, and H_2 on the metal surface, even under ultrahigh vacuum (UHV) conditions [10–15].

Many theoretical studies have been performed to clarify the reaction mechanism of methanol dehydrogenation on metal surfaces because of its importance in DMFCs. Kua and Goddard performed pioneering work by examining the thermostability of the intermediates on 2nd and 3rd row Group VIII metals [16]. They provided important and useful information by executing extensive calculations using a cluster model but the activation energies were not given. Ishikawa et al. have also reported a thermostability analysis by using quasirelativistic density-functional theory (DFT)

* Corresponding author. Present address: Institute for Molecular Science, 38 Nishigo-Naka, Myodaiji, Okazaki 444-8585, Japan. Tel.: +81 564 55 7461; fax: +81 564 55 7025.
E-mail address: ehara@ims.ac.jp (M. Ehara).
[1] Present address: Toyota Central R&D Labs, Inc., Nagakute, Aichi 480-1192, Japan.

0039-6028/$ - see front matter © 2009 Elsevier B.V. All rights reserved.
doi:10.1016/j.susc.2009.01.003

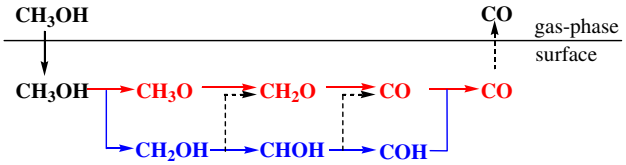

Fig. 1. Reaction pathways of the dehydrogenation reaction from CH_3OH to CO.

calculations of the Xα functional [17]. They also estimated the activation energies, as well as the adsorption and dissociation energies. Desai et al. examined the O–H and C–H bond activations of this reaction using a slab-model [18]. Okamoto et al. investigated this reaction using periodic slab-model DFT calculations, considering the hydrogen-bond network of the solvent water [19]. They reported that in the C–H scission mechanism, the solvent effect is about 0.7 eV for the exothermicity of complete dehydrogenation. Cao et al. [20] and Hartnig and Spohr [21] also studied the solvent effect of water using DFT calculations. Greeley and Mavrikakis performed slab-model DFT calculations to examine the reaction pathways starting with O–H [22] and C–H [23] scission and concluded that C–H scission is dominant, although O–H scission is another realistic route [22,23].

In this situation, we believe that the mechanism of this reaction should be examined, taking into account the electron transfer from the bulk metal and calculating activation energies by locating the transition states (TS). Thus, in the present work, we have investigated the overall reaction pathways of the dehydrogenation reaction of CH_3OH on the Pt surface, using the dipped adcluster model (DAM) [24–26]. The DAM can describe electron exchange between adsorbates and bulk metal (usually electron flows from bulk metal to adsorbates), which is relevant in reactions on metal surfaces. Previously, we investigated the reaction mechanism of CO_2 hydrogenation on the Cu(100) surface, which is related to the present reaction, using the DAM [27]. In this work, we examine the reaction pathway starting from O–H bond scission and compare it with that from C–H bond scission. We have also studied the possibility of methanol dehydrogenation on an Ag surface. We have also examined the cluster size dependence of the results using DAM model.

Recently, the reactions on the nanoscale clusters and nanorods have also been paid much attentions and focused because of their characteristic reactivities [28,29]. The present results are also of interest in view of the reactions on the nanoscale clusters and nanorods. We have also discussed the present reaction in this aspect by examining the standard cluster model.

2. Computational details

The DAM [24,25] was adopted to describe electron exchange between adsorbates and the metal surface. DFT calculations using the B3LYP functional were executed according to the DAM. We also included energy correction due to the image force on the metal surface [26]. We assumed the highest spin coupling model and one-electron transfer from the bulk metal to the adcluster. In the present case, the paired spin coupling is more suitable since the spin-polarization is not experimentally observed for the Pt and Ag surfaces. We adopted, however, the highest spin coupling since it provides stable energy and is computationally simple compared to the paired spin coupling. In the calculations, the spin state of the adcluster was taken as singlet or doublet depending on the step of the reaction.

For the computational model of the Pt surface, we adopted a linear Pt_4 DAM cluster to represent the Pt(111) surface. For the first step which is relevant for the reaction mechanism, we examined the larger clusters for DAM, that is Pt_{10} and Pt_{15} models. The Pt–Pt distance was fixed to 2.772 Å on the basis of the lattice constant of the Pt(111) surface [30]. Most of the structures of the intermediates and transition states have been restricted to C_s symmetry, except for the transition state between CH_2O_a and CHO_a (subscript 'a' indicates a surface-adsorbed species). It was confirmed that all the intermediates are true local minima, and vibrational analysis showed that all the transition states have only one imaginary frequency, except for some states noted. Similarly, the computational model of the Ag surface was also an Ag_4 DAM cluster and the Ag–Ag distance was fixed to 2.892 Å [30]. All calculations were performed using the Gaussian03 suite of programs [31]. The basis set of the Pt atom was (8s6p3d)/ [3s3p2d] and the [Xe] $4f^{14}$ core was replaced by the effective core potential [32]. For carbon, oxygen, and hydrogen atoms, we adopted the Huzinaga–Dunning double zeta polarization [33] plus diffuse s, p functions, that is, (10s6p1d)/[3s3p1d] for C and O atoms, and (5s1p)/[3s1p] for H atoms. The exponents of the diffuse s, p functions were taken from Dunning [34]. For all the steps, we calculated the reaction paths with the standard cluster model to examine the present dehydrogenation reaction on the nanoscale clusters and nanorods. These calculations also show the effect of the electron transfer from bulk metal to the adcluster region.

3. Results and discussion

3.1. Reaction of methanol to form CO starting from O–H bond scission

Fig. 2a shows the energy diagram for the reaction of methanol, from adsorption to dissociation of the O–H bond, producing adsorbed methoxy. The structures of the adsorbed methanol, transition state, and the adsorbed methoxy are also shown. Methanol adsorbs with oxygen at a on-top site of the Pt surface, which agrees with the previous works [18,22]. The adsorption energy of methanol on the Pt surface was calculated to be 11.7 kcal/mol, which is in

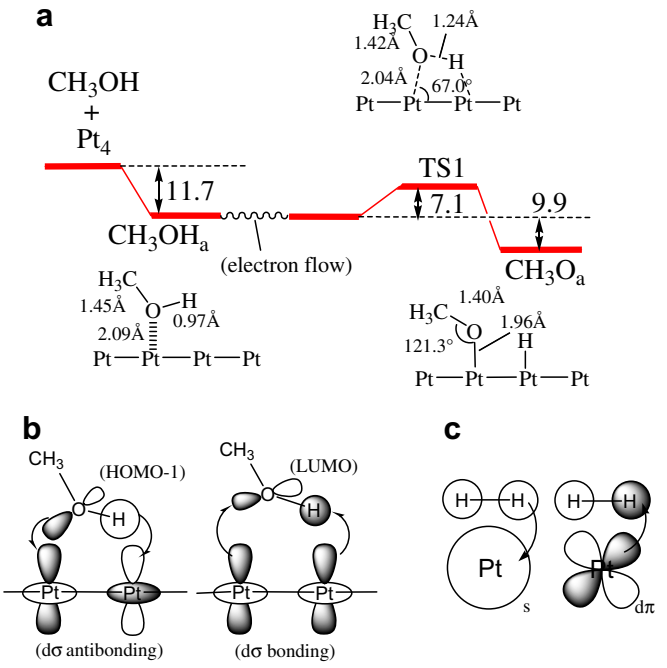

Fig. 2. (a) Energy diagram and optimized geometries for the reaction step from methanol to adsorbed methoxy on the Pt surface (energy in kcal/mol), (b) orbital interaction between methanol and the Pt surface, and (c) orbital interaction in the dissociation of H_2 on the Pt surface [34].

good agreement with the experimental value of 11.4 kcal/mol [35]. The DFT calculations with slab-model gave the adsorption energy as 9.0 kcal/mol [22] and 12.2 kcal/mol [18]. We adopted the model in which electron flow occurs from bulk to adcluster after methanol adsorption. This electron flow occurs because of the stabilization of the adcluster due to the electron-withdrawing methanol adsorption. We do not discuss the electrocatalysis where the electron flow occurs in the opposite direction in this work. Scission of the O–H bond on the Pt surface follows adsorption, with the low energy barrier of 7.1 kcal/mol. This step was calculated to be exothermic by 9.9 kcal/mol. In the slab-model calculations, this step was endothermic by 16–17 kcal/mol [18,22] with the activation energy of 22.0 kcal/mol. The slab-model calculations were executed with the 3×3 unit cell in which the influence of the adjacent unit cell may not be negligible and the results may not converge and also with the plane-wave basis sets. The present DAM calculations included the effect of the bulk by considering electron flow and the calculations were executed with the Gaussian basis sets that are suitable for describing the local phenomena like chemical reactions on the surface. In order to look into the difference of the results in more details, we examined the larger clusters, Pt_{10} and Pt_{15} as discussed later. Two types of orbital interaction stabilize the transition state, that is, out-of-phase and in-phase Pt_2-dσ (d_z^2) orbitals interact with σ(O–H) (HOMO-1) and σ^*(O–H) (LUMO) orbitals, respectively, as depicted in Fig. 2b. In the beginning of the O–H scission, the former donative interaction is dominant, as the orbital energy difference between Pt_2-dσ antibonding and σ(O–H) orbitals is small. In the course of the reaction, the latter back-donation becomes predominant and causes O–H bond cleavage. It should be noted that this type of orbital interaction is characteristic, compared with H_2 dissociation on the Pt surface; the Pt s orbital interacts with $\sigma(H_2)$ in a donative fashion, while the Pt dπ orbital interacts with the $\sigma^*(H_2)$ orbital as in Fig. 2c [36]. For the O-H scission step, the cluster model calculation without electron flow gave almost the same energy barrier (6.1 kcal/mol) and exothermicity (2.9 kcal/mol). This means that the first step of the present reaction may proceed in the same mechanism on the nanoscale clusters and nanorods.

An energy diagram for the reaction step from adsorbed methoxy to formaldehyde is shown, with the structures of the intermediates and transition state, in Fig. 3. The C–H bond dissociates with an activation barrier of 4.4 kcal/mol in agreement with the previous calculations [22]. The orbital interactions of this step are similar to those of the O–H bond scission, and the donative and back-donative interactions involving Pt-dσ orbitals take place. After Pt–H bond formation, both carbon and oxygen coordinate to different Pt atoms and adsorbed formaldehyde forms; the stabilization energy was calculated to be as large as 50.2 kcal/mol. The calculated C–O bond length of this adsorbed formaldehyde is 1.40 Å, which is 0.2 Å larger than in the free molecule. In the previous calculation, the exothermic energy was 9.8 kcal/mol and the C-O bond length was shorter as 1.34 Å [22].

The results for the reaction step from adsorbed formaldehyde to formyl via TS3 are shown in Fig. 4. In this step, we adopted the mechanism in which adsorbed formaldehyde rotates on the Pt surface and Pt–H bond formation occurs. Because we failed to locate the transition state strictly, the energy barrier was calculated by partial optimization, varying the dissociating C–H bond length parameter while the Pt–Pt–C angle and Pt–C bond length were fixed. For this step, a higher activation energy of about 19 kcal/mol was obtained. This is partly because the adsorbed formaldehyde is very stable on the Pt surface, with C–Pt and O–Pt coordinations. Electron transfer is important for this step, which is included in the present DAM calculation: the standard cluster model without electron transfer calculated an energy barrier of 43 kcal/mol. Thus, in the case of the nanoscale clusters and nanorods, it may be possible that the present dehydrogeneation reaction terminates at this step and the formaldehyde is produced. Experimental work reported that defects or steps on the Pt surface change the reaction kinetics [13]. This may indicate that defects or steps destabilize formaldehyde adsorbate and change the energetics of the reaction. The C–O bond length changes from formaldehyde to TS3. Finally, adsorbed formyl was stabilized by 22.3 kcal/mol with both C–Pt and O–Pt coordinations.

For the reaction step that leads from adsorbed formyl to CO via TS4, lower activation energy of about 15 kcal/mol was calculated, as shown in Fig. 5. The C–O bond length shrinks and C–Pt is slightly

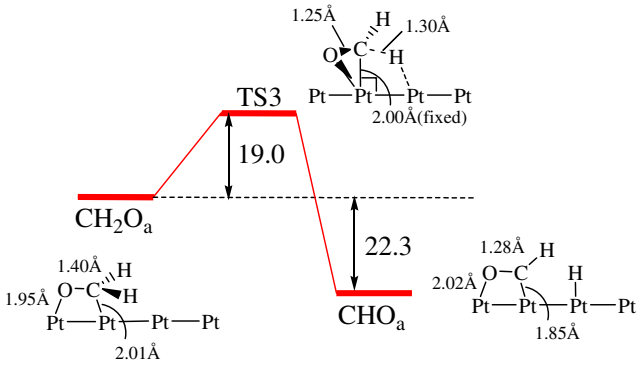

Fig. 4. Energy diagram and optimized geometries for the reaction step from adsorbed formaldehyde to formyl (energy in kcal/mol).

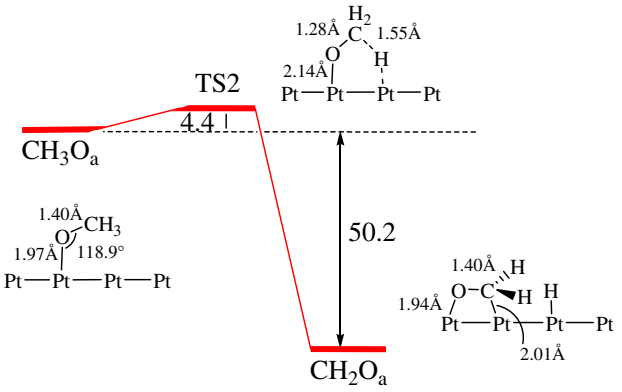

Fig. 3. Energy diagram and optimized geometries for the reaction step from adsorbed methoxy to formaldehyde (energy in kcal/mol).

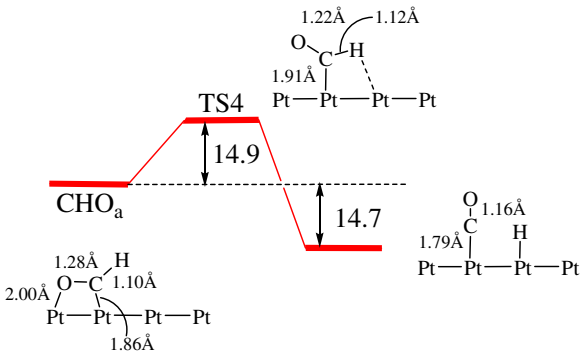

Fig. 5. Energy diagram and optimized geometries for the reaction step from adsorbed formyl to CO (energy in kcal/mol).

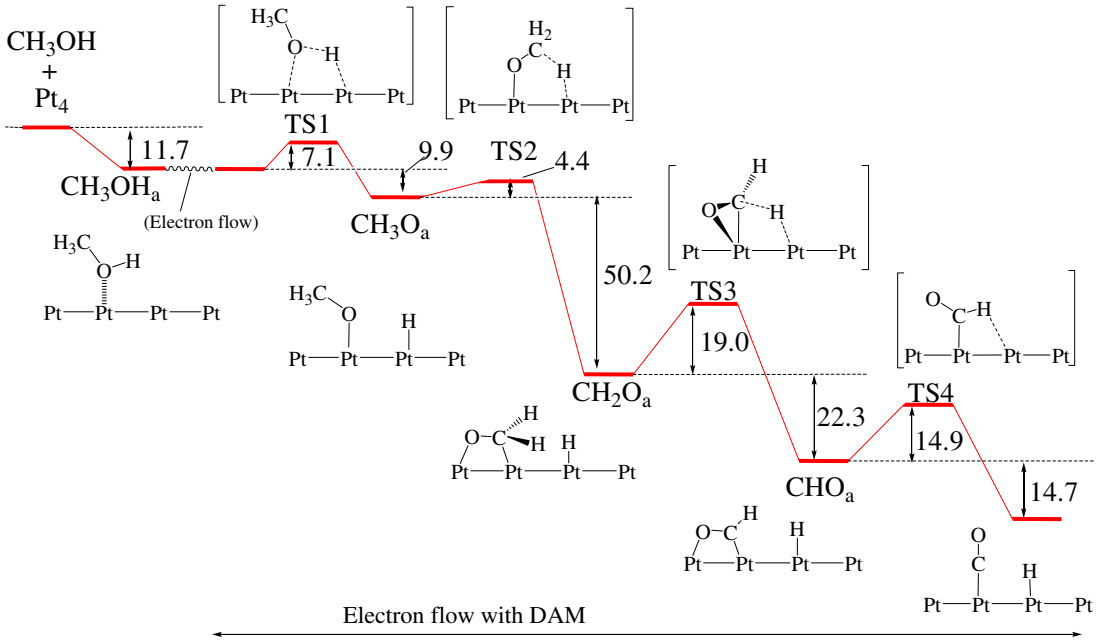

Fig. 6. Overall energy diagram of methanol dehydrogenation starting from O–H bond scission.

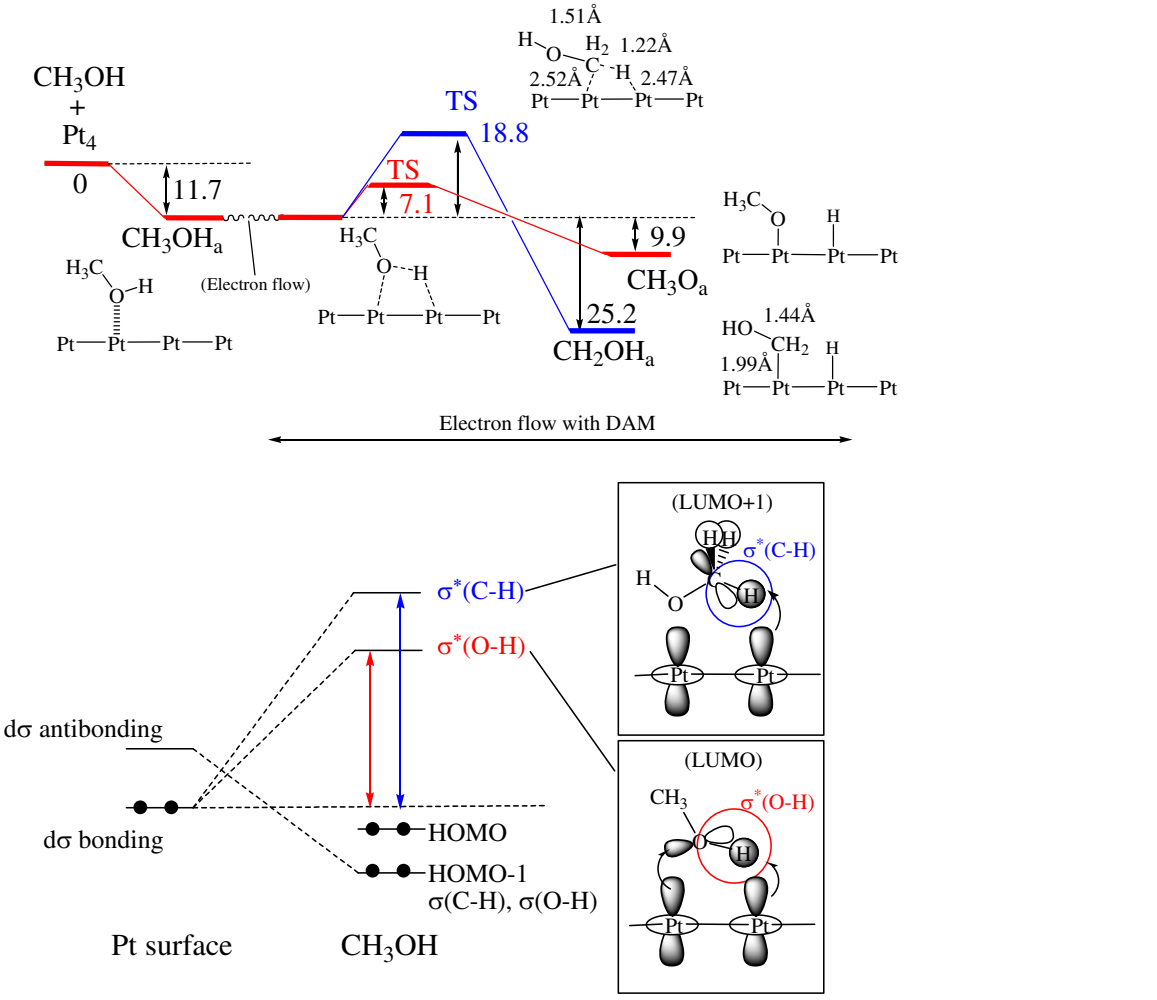

Fig. 7. (a) Comparison of energy diagrams for the reaction pathways starting from the O–H (red) and C–H (blue) scission and (b) orbital interactions of the two reaction pathways (For interpretation of the references to colour in this figure legend, the reader is referred to the web version of this article.).

elongated in TS4. Again, the dσ orbital interaction of Pt with the C–H antibonding orbital stabilizes this TS4. The adsorbed CO was stable at an on-top site and 14.7 kcal/mol more stable than the formyl adsorbate. The resultant CO is further oxidized to CO_2 by the oxidizing agent OH, which is provided from H_2O. This "bifunctional mechanism" was proposed by Watanabe et al. [37]. In the slab-model calculation, this step was calculated to be exothermic by 26.4 kcal/mol with the activation energy of 6.2 kcal/mol [22].

The energy diagram for the overall reaction from methanol to CO on the Pt surface is shown in Fig. 6. The reaction starting from O–H bond scission on the Pt surface was exothermic. A large activation barrier was predicted for the dehydrogenation of formaldehyde to formyl adsorbate.

3.2. Comparison of O–H and C–H scission

In previous works, the reaction pathway starting from C–H scission has been investigated intensively. We also examined this reaction pathway in order to compare it with the pathway starting from O–H scission. The energy diagram for the initial step in these two reaction pathways, that is, the conversion from CH_3OH_a to CH_3O_a or CH_2OH_a, is shown in Fig. 7a. The red line shows the energetics of the O–H bond scission and the blue line indicates those of the C–H bond scission.

The intermediate CH_2OH_a provided by C–H scission is more thermodynamically stable than the CH_3O_a obtained from O–H scission. This fact is well known from previous theoretical studies. For this C–H scission, a high activation energy of about 19 kcal/mol was calculated, which was also obtained in the previous slab-model calculations [22]: the structure of the TS is almost the same to that predicted by the previous calculations. On the other hand, the O–H scission pathway has a lower activation barrier of 7.1 kcal/mol. Therefore, the reaction starting from O–H scission is kinetically more favorable than that starting from C–H scission. The activation energy of the O-H scission calculated by the slab-model was 22.0 kcal/mol, which suggested the C–H scission is favorable pathway [22].

The difference in activation energies between O–H bond scission and C–H bond scission can be interpreted as follows. Based on frontier orbital theory, the stabilization energy of orbital interaction is approximated to be inversely proportional to the orbital energy difference. Fig. 7b shows the schematic orbital interaction between methanol and the Pt surface. The HOMO-1 of methanol has both σ(O–H) and σ(C–H) natures and, therefore, the stabilization caused by donative interaction with Pt-dσ* is nearly the same for both possible pathways. On the other hand, in the back-donative interaction between the Pt-dσ orbital and the methanol antibonding orbital, the σ*(O–H) LUMO is lower than the σ*(C–H) LUMO+1. Thus, O–H scission gains more stabilization energy than C–H scission because of this back-donative interaction.

As noted above, the present results differ from those obtained by the previous slab-model calculations [18,22]. Therefore, we examined the larger Pt_{10} and Pt_{15} models to see the cluster size dependence of our calculations. In these calculations, we did not perform the geometry optimization and used the structures obtained by the Pt_4 model. The results using the Pt_4, Pt_{10} and Pt_{15} models are compared in Fig. 8. In all of these models, the O–H scission is more preferable than the C–H scission: the activation barrier of the O–H scission is lower than that of the C–H scission, although the CH_2OH intermediate is more stable than the methoxy intermediate. The activation energies did not converge in these calculations partly because we did not perform the optimization and the coordination of the second layer metals influenced the bonding nature. The repulsive interaction between adsorbates was large so that we adopted the model that the hydrogen atom migrates rapidly after the reaction by using the separate clusters for this step.

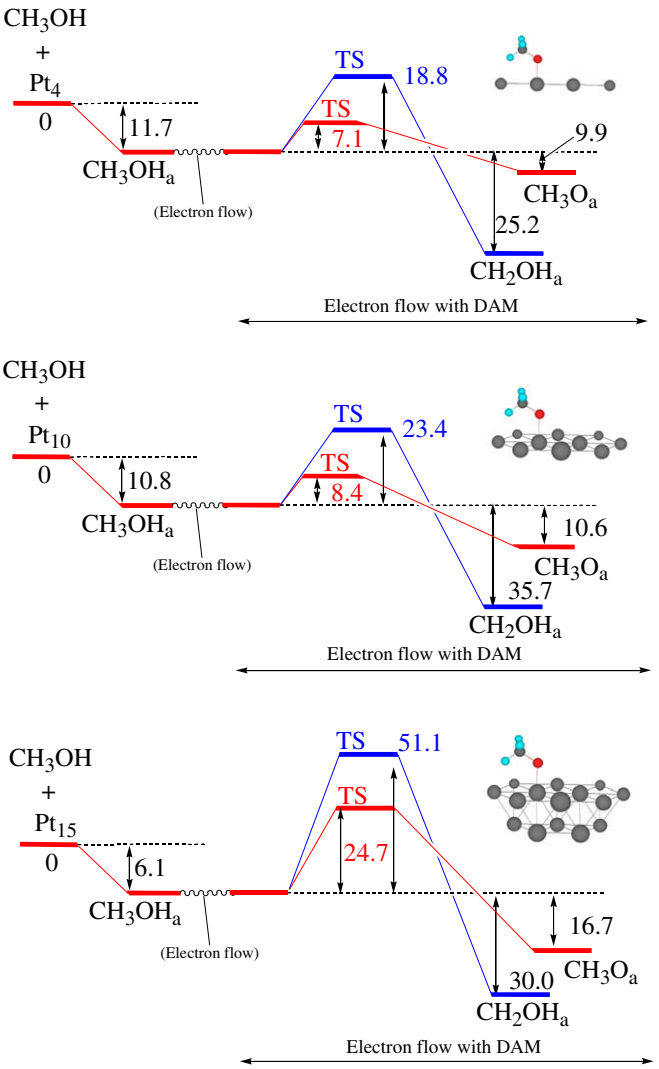

Fig. 8. Comparison of energy diagrams of the first step with (a) Pt_4, (b) Pt_{10}, and Pt_{15} models (energy in kcal/mol).

The O–H scission mechanism was proposed following experiments under ultrahigh vacuum conditions using electron energy-loss spectroscopy (EELS) with an isotope substitution method [10]. Methoxy intermediate was also detected using temperature-programmed desorption (TPD) and EELS [11,38].

3.3. Dehydrogenation on Ag surface

Methanol dehydrogenation on an Ag surface has also been investigated. The reaction pathway starting from O–H scission was examined and the resultant energy diagram up to formaldehyde generation is shown in Fig. 9. The stable geometries of the adsorbed methanol and methoxy species were obtained and the reaction was calculated to be facile, with an activation barrier of 3.6 kcal/mol. The structure of adsorbed methanol and the orbital interaction with the Ag surface accord with the previous study [39]. The energy barrier for formation of formaldehyde was estimated to be slightly larger than 12 kcal/mol, using the partial optimization technique described above.

The stable structure of adsorbed formaldehyde was not obtained for the Ag surface because the potential energy curve of this adsorption was found to be repulsive. The product formaldehyde desorbs from the Ag surface, meaning that the Ag surface is more

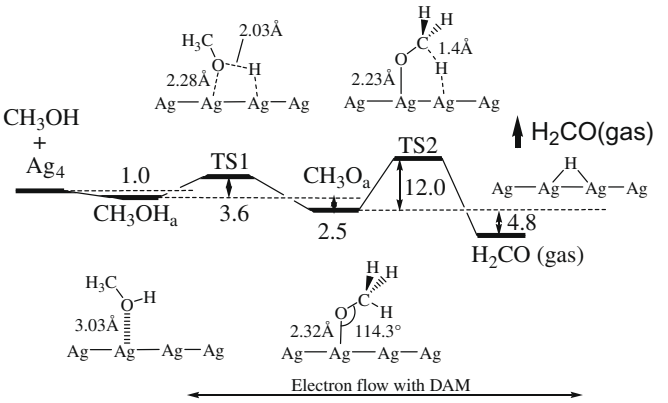

Fig. 9. Energy diagram and optimized geometries for the dehydrogenation of methanol on the Ag surface (energy in kcal/mol).

suitable for formaldehyde synthesis. It is also recognized experimentally that the probability of adsorption of formaldehyde on a clean Ag surface is very small [40]. This characteristic is unique, compared with the Pt surface upon which adsorbed formaldehyde is very stable. In the case of the Pt surface, orbital interaction between Pt-dσ/H_2CO π^* and Pt-dσ/H_2CO π(in-plane) is effective. On the other hand, the HOMO and LUMO of formaldehyde are symmetrically inappropriate for effective interaction with the Ag surface.

4. Summary

We have investigated the mechanism of the methanol dehydrogenation reaction on a Pt surface that is relevant in the DMFC. The reaction pathway starting from O–H bond scission was predicted to be more favorable than that starting from C–H bond scission. The overall reaction pathway from methanol to CO, starting from O–H bond scission, was examined. The donative interaction of the Pt-dσ orbitals was found to be important for catalytic activation on the Pt surface. The Ag surface was found to favor formaldehyde synthesis rather than dehydrogenation to CO. The present calculations adopted the DAM, which describes electron transfer from the bulk metal. Electron transfer from the metal surface is important in particular for the energy barrier of the dehydrogenation of formaldehyde. The present results suggested that the reaction also occurs on the nanoscale clusters and nanorods in the same mechanism but terminates at the formaldehyde.

Acknowledgments

We would like to thank the reviewers for their valuable comments. This study was supported by JST, CREST and a Grant-in-Aid for Scientific Research in Priority Areas "Molecular Theory for Real Systems" from the Ministry of Education, Culture, Sports, Science and Technology of Japan. The computations were performed using Research Center for Computational Science, Okazaki, Japan.

References

[1] H.A. Wittcoff, G.B. Reuben, Industrial Organic Chemicals, Wiley, New York, 1996.
[2] A.P.V. Soares, M.F. Portela, Catal. Rev. 47 (2005) 125.
[3] A. Hammett, Catal. Today 38 (1997) 445.
[4] K.R. Williams, G.T. Burstein, Catal. Today 38 (1997) 401.
[5] G.T. Burstein, C.J. Barnett, A.R. Kucemak, K.R. Williams, Catal. Today 38 (1997) 425.
[6] T. Hatanaka, R&D Review of Toyota CRDL 37 (2001) 59.
[7] Y. Kubo, H. Imai, Hyomen bussei kogaku handbook, second ed., Maruzen, Tokyo, 2006 (chapter 21).
[8] J.L. Davis, M.A. Barteau, Surf. Sci. 187 (1987) 387.
[9] V.S. Bagotzky, Y.B. Vassiliev, O.A. Khazova, J. Electroanal. Chem. 81 (1977) 229.
[10] K. Franaszczuk, E. Herrero, P. Zelenay, A. Wieckowski, J. Wang, R.I. Masel, J. Phys. Chem. 96 (1992) 8509.
[11] J. Wang, R.I. Masel, Surf. Sci. 243 (1990) 199.
[12] Y.X. Chen, A. Miki, S. Ye, H. Sakai, M. Osawa, J. Am. Chem. Soc. 125 (2003) 3680.
[13] K.D. Gibson, L.H. Dubois, Surf. Sci. 233 (1990) 59.
[14] D.H. Ehlers, A. Spitzer, H. Lu-th, Surf. Sci. 160 (1985) 57.
[15] B.A. Sexton, Surf. Sci. 102 (1981) 271.
[16] J. Kua, W.A. Goddard III, J. Am. Chem. Soc. 121 (1999) 10928.
[17] Y. Ishikawa, M.-S. Liao, C.R. Cabrera, Surf. Sci. 463 (2000) 66.
[18] S.K. Desai, M. Neurock, K. Kourtakis, J. Phys. Chem. B 106 (2002) 2559.
[19] Y. Okamoto, O. Sugino, Y. Mochizuki, T. Ikeshoji, Y. Morikawa, Chem. Phys. Lett. 377 (2003) 236.
[20] D. Cao, G.-Q. Lu, A. Wieckowski, S.A. Wasileski, M. Neurock, J. Phys. Chem. B 109 (2005) 11622.
[21] C. Hartnig, E. Spohr, Chem. Phys. 319 (2005) 185.
[22] J. Greeley, M. Mavrikakis, J. Am. Chem. Soc. 124 (2002) 7193.
[23] J. Greeley, M. Mavrikakis, J. Am. Chem. Soc. 126 (2004) 3910.
[24] H. Nakatsuji, J. Chem. Phys. 87 (1987) 4995.
[25] H. Nakatsuji, Progress in Surface Science 54 (1997) 1.
[26] H. Nakatsuji, H. Nakai, Y. Fukunishi, J. Chem. Phys. 95 (1991) 640.
[27] Z.-M. Hu, K. Takahashi, H. Nakatsuji, Surf. Sci. 442 (1999) 90.
[28] Y. Okamoto, Chem. Phys. Lett. 429 (2006) 209.
[29] F. Liu, J.Y. Lee, W.J. Zhou, Small 2 (2006) 121.
[30] C. Kittel, Introduction to Solid State Physics, seventh ed., Wiley, New York, 1998.
[31] M.J. Frisch, G.W. Trucks, H.B. Schlegel, G.E. Scuseria, M.A. Robb, J.R. Cheeseman, J.A. Montgomery Jr., T. Vreven, K.N. Kudin, J.C. Burant, J.M. Millam, S.S. Iyengar, J. Tomasi, V. Barone, B. Mennucci, M. Cossi, G. Scalmani, N. Rega, G.A. Petersson, H. Nakatsuji, M. Hada, M. Ehara, K. Toyota, R. Fukuda, J. Hasegawa, M. Ishida, T. Nakajima, Y. Honda, O. Kitao, H. Nakai, M. Klene, X. Li, J.E. Knox, H.P. Hratchian, J.B. Cross, C. Adamo, J. Jaramillo, R. Gomperts, R.E. Stratmann, O. Yazyev, A.J. Austin, R. Cammi, C. Pomelli, J.W. Ochterski, P.Y. Ayala, K. Morokuma, G.A. Voth, P. Salvador, J.J. Dannenberg, V.G. Zakrzewski, S. Dapprich, A.D. Daniels, M.C. Strain, O. Farkas, D.K. Malick, A.D. Rabuck, K. Raghavachari, J.B. Foresman, J.V. Ortiz, Q. Cui, A.G. Baboul, S. Clifford, J. Cioslowski, B.B. Stefanov, G. Liu, A. Liashenko, P. Piskorz, I. Komaromi, R.L. Martin, D.J. Fox, T. Keith, M.A. Al-Laham, C.Y. Peng, A. Nanayakkara, M. Challacombe, P.M.W. Gill, B. Johnson, W. Chen, M.W. Wong, C. Gonzalez, J.A. Pople, Gaussian 03, Gaussian Inc., Pittsburgh PA, 2003.
[32] P.J. Hay, W.R. Wadt, J. Chem. Phys. 82 (1985) 270.
[33] S. Huzinaga, J. Chem. Phys. 42 (1965) 1293.
[34] T.H. Dunning Jr., P.J. Hay, Modern Theoretical Chemistry, Plenum, New York, 1976.
[35] B.A. Sexton, A.E. Hughes, Surf. Sci. 140 (1984) 227.
[36] H. Nakatsuji, Y. Matsuzaki, T. Yonezawa, J. Chem. Phys. 88 (1988) 5759.
[37] M. Watanabe, S. Motoo, J. Electroanal. Chem. 60 (1975) 267.
[38] N. Kizhakevariam, E.M. Stuve, Surf. Sci. 286 (1993) 246.
[39] M. Voss, D. Borgmann, G. Wedler, Surf. Sci. 465 (2000) 211.
[40] L.E. Fleck, Z.C. Ying, M. Feehery, H.L. Dai, Surf. Sci. 296 (1993) 400.